PCCP

Thermal decomposition of cyclohexane by flash pyrolysis vacuum ultraviolet photoionization time-of-flight mass spectrometry: A study on the initial unimolecular decomposition mechanism

Journal:	*Physical Chemistry Chemical Physics*
Manuscript ID	CP-ART-02-2021-000459.R1
Article Type:	Paper
Date Submitted by the Author:	30-Mar-2021
Complete List of Authors:	Shao, Kuanliang; University of California, Department of Chemistry Liu, Xinghua; Hainan University Jones, Paul; University of California, Department of Chemistry Sun, Ge; University of California, Department of Chemistry Gomez, Mariah; University of California Los Angeles Riser, Blake; University of California, Department of Chemistry Zhang, Jingsong; University of California, Department of Chemistry

Thermal decomposition of cyclohexane by flash pyrolysis vacuum ultraviolet photoionization time-of-flight mass spectrometry: A study on the initial unimolecular decomposition mechanism

Kuanliang Shao, Xinghua Liu,[a] Paul J. Jones, Ge Sun, Mariah Gomez,[b] Blake P. Riser, and Jingsong Zhang*

Department of Chemistry

University of California, Riverside

California 92521, United States

Abstract

Thermal decomposition of cyclohexane at temperatures up to 1310 K was performed using flash pyrolysis coupled with vacuum ultraviolet (118.2 nm) photoionization time-of-flight mass spectrometry. The experimental results revealed that the major initiation reaction of cyclohexane decomposition was C-C bond fission leading to the formation of 1,6-hexyl diradical. The 1,6-hexyl diradical could isomerize to 1-hexene and decompose into $\bullet C_3H_7$ + $\bullet C_3H_5$ and $\bullet C_4H_7$ + $\bullet C_2H_5$. The 1,6-hexyl diradical could also undergo direct dissociation; the C_4H_8 fragment via the 1,4-butyl diradical intermediate was observed, serving as evidence of the 1,6-hexyl diradical mechanism. Quantum chemistry calculations at UCCSD(T)/cc-pVDZ level of theory on the initial

reaction pathways of cyclohexane were performed and found to be consistent with the experimental conclusions. Cyclohexyl radical was not observed as an initial intermediate in the pyrolysis. Benzene was produced from sequential H_2 eliminations of cyclohexane at high temperatures.

Keywords: Mass spectrometry, flash pyrolysis, reaction mechanism, cyclohexane.

---

[a] Current Address: College of Science, Hainan University, Hainan 570228, China.

[b] Current Address: Department of Chemistry and Biochemistry, University of California, Los Angeles, California 90095, USA.

[*] Corresponding author. Email: jingsong.zhang@ucr.edu; Tel +1 951 827 4197; Fax: +1 951 827 4713. Also at Air Pollution Research Center, University of California, Riverside, California 92521, USA.

Introduction

Cycloalkanes and their thermal decompositions are ubiquitous in hydrocarbon fuel usage and biomass conversion.[1-5] Cyclohexane, for its relatively simple structure, has been considered as a prototypical cycloalkane system. The pyrolysis of cyclohexane has been extensively studied experimentally and theoretically. In a single-pulse shock-tube study, Tsang stated that the main initial steps involve isomerization of cyclohexane (c-C_6H_{12}) to 1-hexene (1-C_6H_{12}) through a diradical intermediate (•$CH_2(CH_2)_4H_2C$•), followed by decomposition of 1-hexene to •C_3H_7 and •C_3H_5 (reaction (1)-(2)). They argued that C_3H_6 could also be produced from retro-ene dissociation of 1-hexene (reaction (3)).[6] Brown et al. reported similar results by applying the very low-pressure pyrolysis (VLPP) technique.[7]

$$c\text{-}C_6H_{12} \rightarrow \bullet CH_2(CH_2)_4H_2C\bullet \rightarrow 1\text{-}C_6H_{12} \quad (1)$$

$$1\text{-}C_6H_{12} \rightarrow \bullet C_3H_7 + \bullet C_3H_5 \quad (2)$$

$$1\text{-}C_6H_{12} \rightarrow 2\,C_3H_6 \quad (3)$$

Arikibe et al. developed a numerical kinetic simulation and proposed a detailed mechanism of cyclohexane pyrolysis as shown in Scheme 1.[8, 9] In this model, the reaction is initiated by the fission of C-C single bond forming a diradical intermediate, and then it dissociates to different products, such as $C_4H_8 + C_2H_4$, $C_3H_6 + C_3H_6$ (reaction (4) - (5)) and

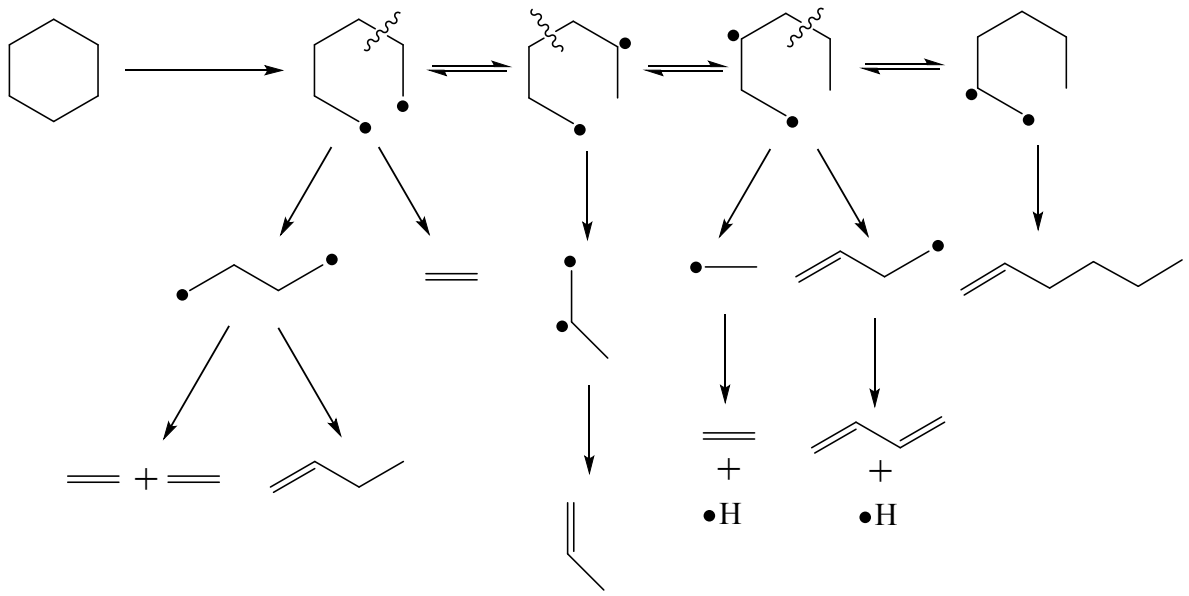

Scheme 1. The reaction mechanism for cyclohexane pyrolysis proposed by Aribike et al.[8,9]

isomerizes to 1-C_6H_{12} (reaction (1)). Bakali et al. examined the oxidation of cyclohexane in a jet-stirred reactor (JSR) at various temperatures and pressures.[10] They added that decomposition of cyclohexane to cyclobutane is an important initiation pathway (reaction (6)). However, the signal of cyclobutane was not detected in that work, as cyclobutane may quickly dissociate to ethylene. The yield of cyclohexyl radical (c-•C_6H_{11}) from c-C_6H_{12} (reaction (7)) was also added to improve the prediction of the 1-hexene concentration profile. Unlike the mechanism proposed by Arikibe et al. (reaction (4)), the recombination reaction of •CH_3 and •C_3H_5 (reaction (8)) was postulated as a pathway for the 1-butene production.

$$c - C_6H_{12} \leftrightarrow \bullet CH_2(CH_2)_4H_2C\bullet \rightarrow \bullet CH_2(CH_2)_2H_2C\bullet + C_2H_4 \rightarrow 1 - C_4H_8 + C_2H_4 \quad (4)$$

$$c\text{-}C_6H_{12} \leftrightarrow \bullet CH_2(CH_2)_4H_2C\bullet \rightarrow 2\ CH_2 = CHCH_3$$

(5)

$$c\text{-}C_6H_{12} \rightarrow c\text{-}C_4H_8 + C_2H_4 \quad (6)$$

$$c\text{-}C_6H_{12} \rightarrow c\text{-}\bullet C_6H_{11} + H\bullet \quad (7)$$

$$\bullet CH_3 + \bullet C_3H_5 \rightarrow 1\text{-}C_4H_8 \quad (8)$$

Later, Steil et al. conducted the pyrolysis of cyclohexane using the shock tube technique and argued that there was a 1:1 branching ratio between reaction (7) and reaction (1), and the importance of reaction (7) was previously underestimated.[11] It was also stated that the cyclohexyl radical further loses one H atom to form cyclohexene (reaction (9)), and several subsequent reactions would occur after that. Granata et al. considered that cyclohexene could be produced directly from cyclohexane by H_2 elimination (reaction (10)) in their kinetic modeling of cyclohexane.[12]

$$c\text{-}\bullet C_6H_{11} \rightarrow c\text{-}C_6H_{10} + H\bullet \quad (9)$$

$$c\text{-}C_6H_{12} \rightarrow c\text{-}C_6H_{10} + H_2 \quad (10)$$

Kiefer et al. performed the thermal decomposition of cyclohexane and 1-hexene by applying the shock tube technique as well as numerical modeling.[13] It was considered that 1-hexene was the main initial product in the cyclohexane pyrolysis, and 1-hexene was consumed predominantly via C3-C4 bond fission (reaction (2)). The production of

•C_2H_5 + •C_4H_7 (reaction (11)) and •CH_3 + •C_5H_9 (reaction (12)) were considered to make a marginal contribution to the overall mechanism. The retro-ene reaction (3) was found to be insignificant under their reaction conditions. Liu et al. performed the flash pyrolysis of 1-hexene coupled with vacuum ultraviolet single-photon ionization mass spectrometry (VUV-SPI-MS) and studied its unimolecular decomposition mechanism.[14] They argued that the 1,5-diradical and 1,6-diradical retro-ene reactions leading to the formation of 1,5-hexyl diradical and 1,6-hexyl diradical are important initiation pathways (reaction (13a) and (13b)) in the 1-hexene thermal decomposition. Recently, some other works which mainly focused on improving the rate coefficients to better quantify the mechanistic models have also been reported.[8, 15-18]

$$1\text{-}C_6H_{12} \rightarrow \bullet C_2H_5 + \bullet C_4H_7 \quad (11)$$

$$1\text{-}C_6H_{12} \rightarrow \bullet CH_3 + \bullet C_5H_9 \quad (12)$$

$$1\text{-}C_6H_{12} \rightarrow 1,5\text{-}\bullet C_6H_{12}\bullet \quad (13a)$$

$$1\text{-}C_6H_{12} \rightarrow 1,6\text{-}\bullet C_6H_{12}\bullet \quad (13b)$$

The formation mechanism of the C_6H_6 compounds during the cyclohexane decomposition also drew some attention. Several mechanisms were proposed for the C_6H_6 production. One was a stepwise dehydrogenation mechanism from the parent

precursor,[10, 19-22] and the other was bimolecular recombination reactions of smaller species such as $C_2H_2 + C_4H_4$ or $C_3H_3 + C_3H_3$.[15, 18, 23-25]

In addition to the experimental investigations mentioned above, quantum chemistry studies have also been performed, and the role of the 1,6-hexyl diradical in the cyclohexane pyrolysis was an emphasis. Sirjean et al. reported a theoretical investigation based on CBS-QB3 calculations on the cycloalkane unimolecular dissociations.[26] The Gibbs free energies of each species of interest including the diradical intermediates were calculated. The C-C bond breaking of cyclohexane producing the 1,6-hexyl diradical was considered as the initiation step, and the barrier for the 1,6-hexyl diradical to further dissociate into 1,4-butyl diradical and ethylene was calculated to be 107 kJ/mol. Kiefer et al. examined the thermal decomposition pathways of cyclohexane and 1-hexene at the CASPT2/cc-pVDZ level.[13] They argued that the 1,6-hexyl diradical could be formed from the ring-opening reaction of cyclohexane, and rapidly isomerizes to 1-hexene as other reactions of 1,6-hexyl diradical are not competitive. Gong et al. explored the decomposition mechanism of cyclohexane at the CCSD(T)/cc-pVDZ//UBH&HLYP/cc-pVDZ level of theory. The reaction pathways of the $\bullet C_6H_{12}\bullet$ diradical (both singlet and triplet) yielding the C_4H_8 species as well as other products were studied.[27] Huang et al. performed a density functional theory (DFT) investigation on the decomposition of cyclohexane in the hydrogen plasma at the B3LYP/6-31G(d,p) level of theory.[28] In that work, the 1,6-hexyl diradical was considered to be a less important reaction intermediate,

while the cyclohexane pyrolysis was mainly initiated by C-H bond breaking with the involvement of an active hydrogen atom.

Although many studies on the cyclohexane pyrolysis have been reported, there are still some different opinions on the initial steps. For example, there are questions on the role of the 1,6-hexyl diradical in the cyclohexane decomposition, and if or not it has direct dissociation pathways in the unimolecular reaction regime. In previous works, either the reaction time or the product detection time was long, and therefore the bimolecular reactions could not be avoided; the unimolecular reactivity of the 1,6-hexyl diradical was rather unclear. Other reaction mechanisms such as the formation of the cyclohexyl radical and benzene could also be re-examined under the unimolecular reaction conditions. These motivate further studies to focus on the initial steps of the unimolecular dissociation of cyclohexane. Here, we provide a different approach, using flash pyrolysis of diluted cyclohexane in inert carrier gas (~ 1%) in a short reaction time (< 100 μs), which can mainly focus on the initiation pathways of the unimolecular thermal decomposition of cyclohexane. In this work, evidence for the 1,6-hexyl diradical and its direct dissociation was exhibited. The $\bullet C_6H_{11}$ radical was not detected in this work. Therefore, the initial reactions of cyclohexane were primarily explained by the ring-opening and diradical mechanism. The formation mechanism of the C_6H_6 species was also examined in this work.

Experimental and computational methods

The flash pyrolysis of cyclohexane was carried out by employing a vacuum ultraviolet photoionization time-of-flight mass spectrometer (VUV-PI-TOFMS) coupled with a SiC tubular microreactor, which has been described previously.[29-32] The cyclohexane precursor (99.9%, Fisher Scientific) was diluted to around 1% in the N_2 or helium carrier gas. The gas mixture passed through a pulse valve operated at 10 Hz and expanded into the SiC microreactor. The dimensions of the SiC microreactor were depicted in Scheme 2. It had 1 mm i.d., 2 mm o.d., a total length of 4.3 cm, and a heated region of 1.5 cm. The backing pressure of the gas mixture at the microreactor inlet was 1050 Torr. The pressure within the microreactor experienced a significant decrease.[33, 34] The pulsed gas flow in this work was long enough to fill the entire microreactor, and the gas pressure in the microreactor was high enough to be treated as a continuum flow. The

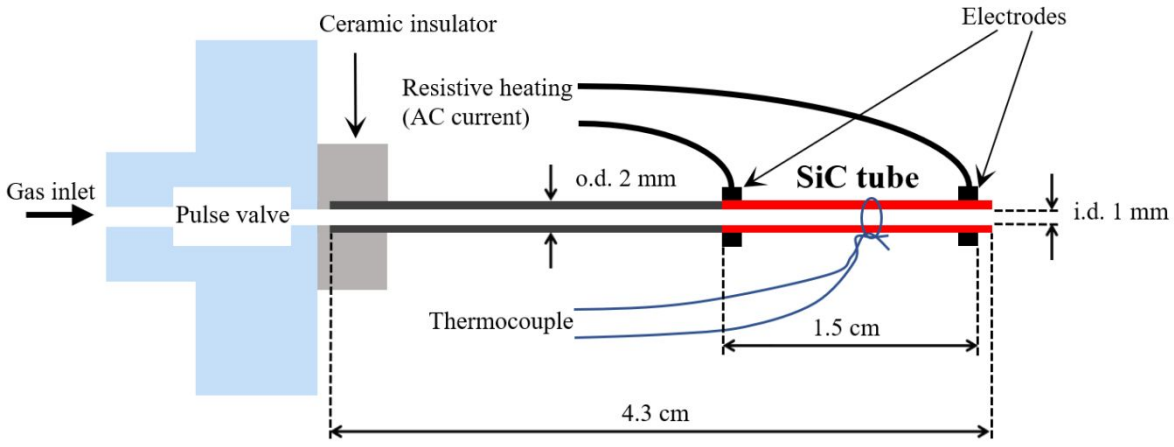

Scheme 2. Schematic diagram of the SiC microreactor.

pressure at the exit of the microreactor was estimated to be around 16 Torr using the continuum flow model reported by Zagidullin et al.[33] The SiC microreactor was heated by an electric current that passed through. The temperature of the nozzle was monitored using an Omega (Type C) thermocouple attached to the outside of the nozzle and calibrated to the internal nozzle temperature.[31] The uncertainty in the temperature measurement was estimated to be ± 50 K. The temperature within the microreactor was expected to be non-uniform along the radial and axial directions,[33, 34] but the temperature measurements can still be used for qualitative analysis. The residence time within the microreactor was estimated to be less than 100 μs.[34] The characterizations of the gas-phase reactions within the SiC tube were similar to those reported before,[33,34-36] with unimolecular decomposition strongly favored and surface and bimolecular reactions minimized.[34] The reaction intermediates, products, and unreacted precursors along with the inert carrier gas then exited the microreactor and supersonically expanded into a molecular beam in the main chamber (at a pressure of ~ 10^{-6} Torr). The molecular beam entered the photoionization zone and was intercepted by a 118.2 nm VUV radiation (10.49 eV). The 118.2 nm VUV laser radiation was produced by tripling the 355 nm Nd:Yag laser radiation in a xenon gas cell at a pressure of ~ 16 Torr. After the photoionization process, ions were accelerated in the TOF mass spectrometer and detected by a multichannel plate detector. The TOF mass spectra were collected by a digital oscilloscope (Tektronix TDS3032, 300 MHz) after signal averaging over 512 laser shots.

Quantum chemistry calculations were also performed on the energies of the reactants, products, and transition states involved in the cyclohexane pyrolysis. Cyclohexane is known for its 3 common conformers: chair, boat, and twist boat. Only the chair conformer, the lowest energy conformer, was chosen because the three have similar energies and relatively small isomerization barriers.[26] For the same reason, only the lowest energy conformer for each diradical was considered. The geometries of species of interest were optimized using the UB3LYP method with the cc-pVDZ basis sets. It could yield reliable geometries compared to those with more advanced computational approaches.[26, 37] All transition states were verified using intrinsic reaction coordinate (IRC) calculations at the UB3LYP/cc-pVDZ level. The single-point energy was calculated using the UCCSD(T) method (with full treatment of single and double excitations and an estimate to the non-iteratively calculated triple excitation contributions) and cc-pVDZ basis sets. The zero-point energy (ZPE) corrections were made based on the frequency calculations at the UB3LYP/cc-pVDZ level. In addition, the energies of singlet diradicals in this work were calculated using $E_{singlet} = 2E_{Guess=Mix} - E_{triplet}$,[38, 39] in which the energy of the diradical with the "Guess=Mix" option was assumed to be the average of the single point energies of its singlet configuration and triplet configuration. This method was first proposed by Ziegler et al in order to deal with the unsatisfactory spin contaminations caused by significant mixing between the singlet and triplet states of diradicals.[27, 38, 39] All vibrational frequencies were scaled by 0.97 in this work as recommended by Sinha et al..[40]

The single-reference calculation approach in this work was similar to the method employed in Gong et al.[27] All the computational works in this work were employed using Gaussian 09 package.[41]

Results and discussions

1. Initiation reactions

The mass spectra of thermal decomposition of cyclohexane from 295 K to 1310 K are presented in Figure 1 and 2. At 295 K, m/z = 84 and 85 correspond to the signal of the cyclohexane parent molecule. The natural isotope abundance of ^{12}C : ^{13}C is 98.9 : 1.1 and H : D = 99.98 : 0.02.[42] The peak area ratio of m/z = 85 to 84 was measured to be 0.083, close to the expected value of 0.074. The ionization energy (IE) of cyclohexane is 9.82 eV,[43] which is lower than the VUV photon energy (10.49 eV). The minor signal of m/z = 56 (C_4H_8) and m/z = 55 (C_4H_7) at 295 K, prior to any contributions from thermal decomposition, were caused by a small amount of multiphoton or electron impact ionization fragmentation of the parent molecule, as the appearance energy of $C_4H_8^+$ and $C_4H_7^+$ in the photoionization of cyclohexane are larger than 10.49 eV.[44] The small amount of electron impact ionization could be resulted from photoelectrons produced by scattered VUV radiation within the photoionization region.[46] At 295 K, m/z = 28 corresponded to the signal of $[N_2]^+$, as N_2 was the inert carrier gas utilized in this cyclohexane pyrolysis. Although the IE of N_2 is 15.6 eV[45] which is higher than 10.49 eV, the minor signal was

due to a small amount of electron impact or multiphoton ionization of the N_2 molecules.[46] As will be discussed later, when the temperature increased, the increase of the m/z = 28 peak could also correspond to the signal of neutral C_2H_4 molecules produced by thermal dissociations. Note that N_2 (m/z = 28.01) and C_2H_4 (m/z = 28.05) mass peaks could not be resolved by the mass spectrometer in this work.

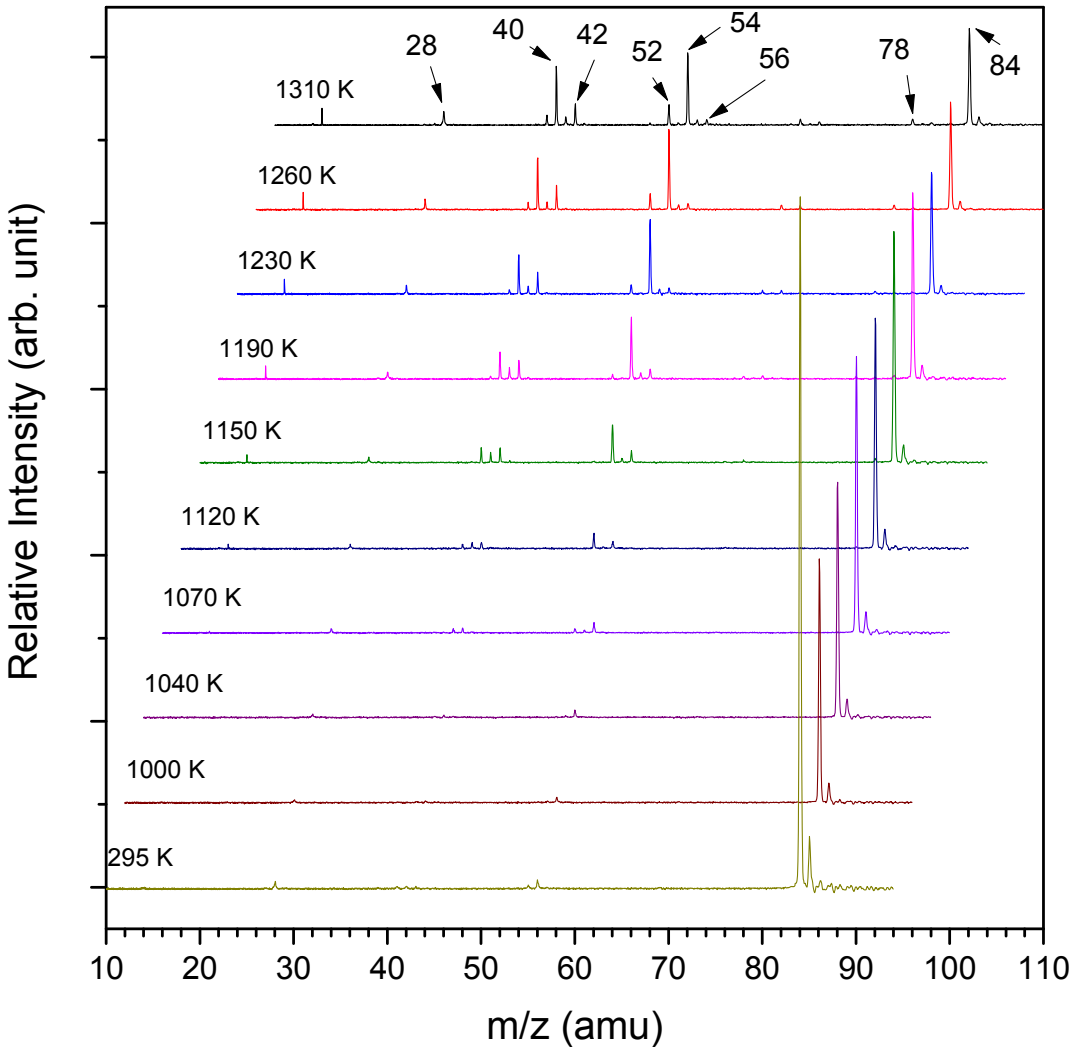

Figure 1. Mass spectra for the cyclohexane pyrolysis at 295 K to 1310 K. Four mass spectra at temperatures between 540 K and 940 K were identical to that at 1000 K and were omitted. The mass spectra are offset horizontally for clarity.

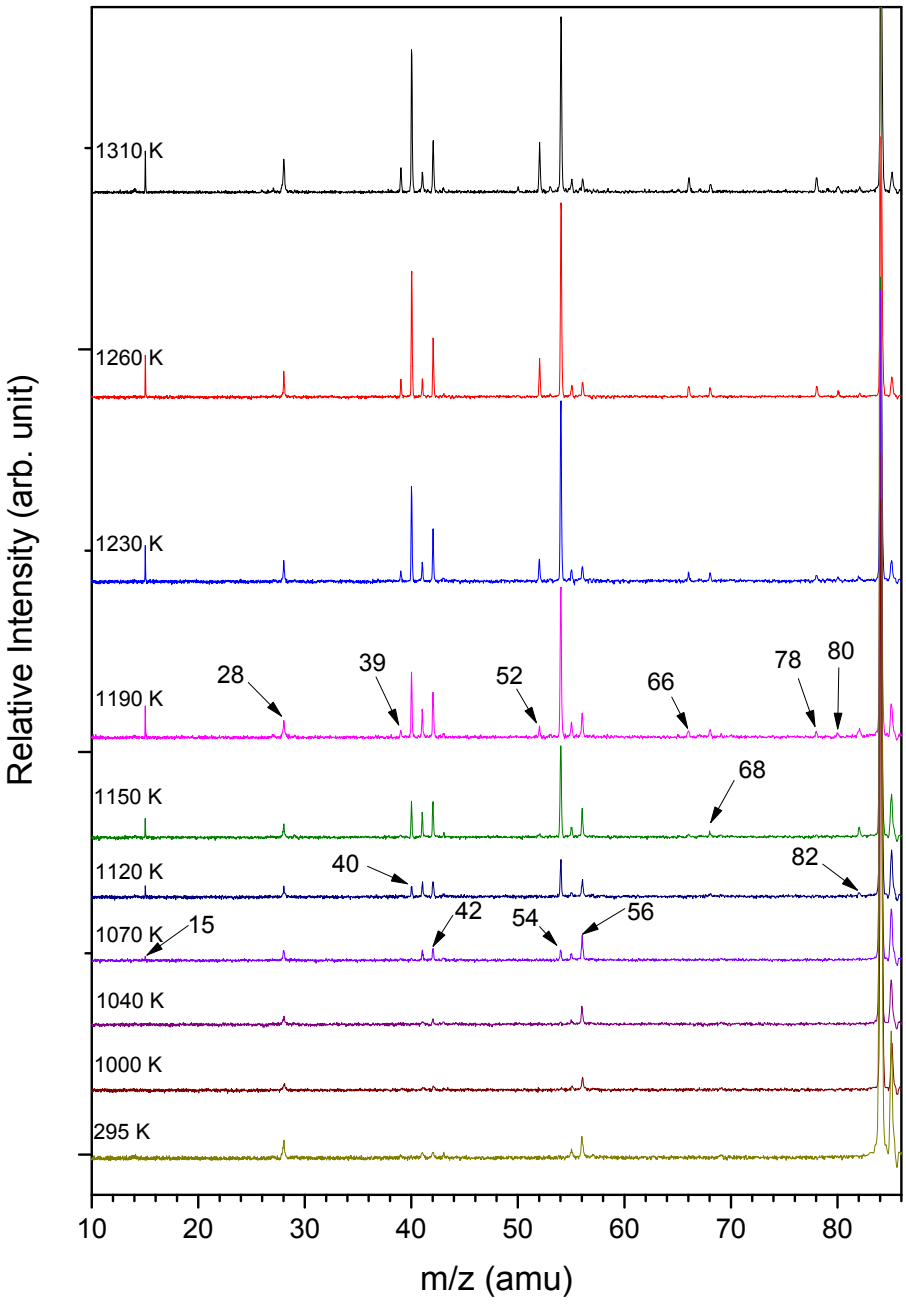

Figure 2. Enlarged sections of mass spectra for the cyclohexane pyrolysis at 295 K to 1310 K. Four mass spectra at temperatures between 540 K and 940 K were identical to that at 1000 K and were omitted. The relative intensity scale is the same for all the mass spectra, but the vertical space is adjusted to better show peaks of fragments at elevated temperatures.

1.1 Formation of the C_4H_8 species

Experimental evidence for the direct dissociation of the 1,6-hexyl diradical was identified. As shown in Figure 1 and 2, the *m*/*z* = 56 peak was detected as a minor ionization fragmentation peak of the parent molecule at 295 K, and it started to increase in intensity at around 1070 K. The signal kept growing until at ~ 1190 K and remained approximately constant as the temperature further increased. To better illustrate the contributions to the signals from thermal decomposition,[29] the ratios of fragment peak areas relative to the parent are plotted for several species in Figure 3**.** The ratio of *m*/*z* =

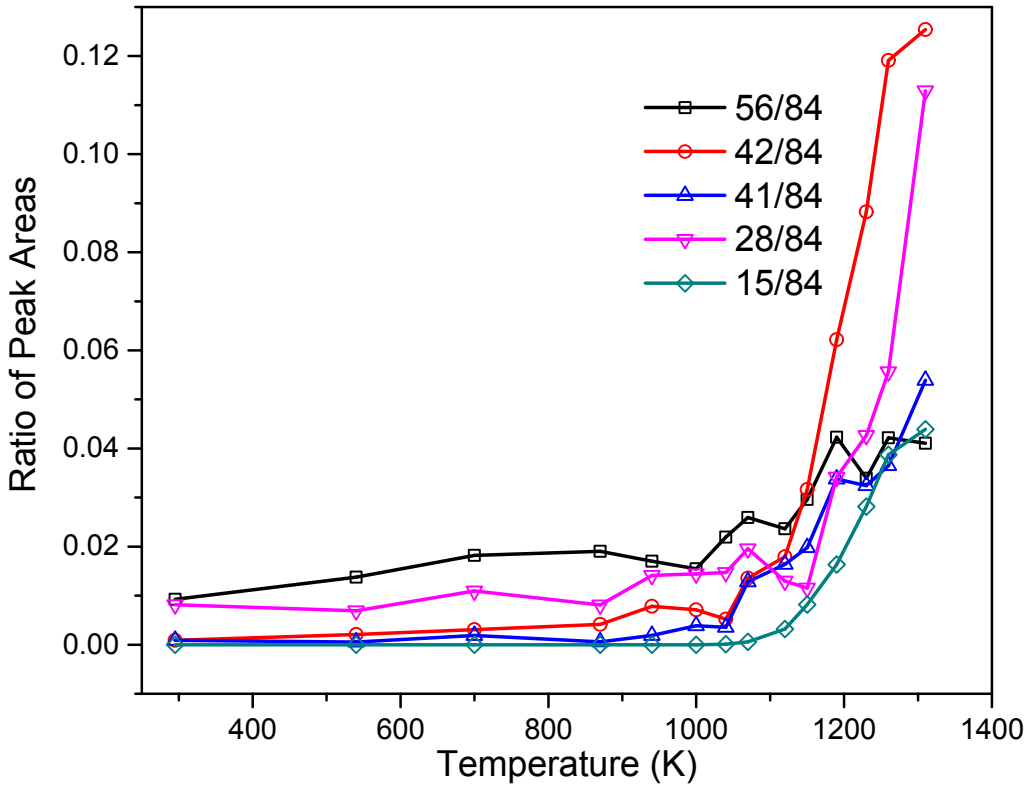

Figure 3. The ratio of peak area of several fragment peaks against the parent peak in the cyclohexane pyrolysis.

56 mass peak area to the parent (*m*/*z* = 84) shows that at around 1070 K, *m*/*z* = 56 peak (C_4H_8) started to grow, and the ratio further increased with the temperature. The reaction (4) is a likely reaction pathway for cyclohexane to decompose into C_4H_8 and C_2H_4 through the 1,6-hexyl diradical intermediate.[9, 14] The absence of *m*/*z* = 57 peak (C_4H_9) at all temperatures suggests that the C_4H_8 species was not produced from H-atom loss from the C_4H_9 radical. This is consistent with Kiefer et al. that the C2-C3 bond fission was not feasible for 1-hexene, which was the major isomerization product following the 1,6-hexyl diradical in the cyclohexane pyrolysis (reaction (1)).[13] Also, since bimolecular reactions were minimized by short reaction time and low precursor concentrations, the bimolecular recombination reaction of $\bullet C_3H_5$ and $\bullet CH_3$ to form C_4H_8 (reaction (8)) was unlikely; furthermore, C_4H_8 was already formed prior to a significant amount of $\bullet C_3H_5$ and $\bullet CH_3$ were produced. Hence, the increase of the *m*/*z* = 56 signal at around 1070 K indicated that C_4H_8 was evolved from breaking of the C2-C3 single bond in the $\bullet C_6H_{12}\bullet$ diradical, and this was also the evidence of the existence of the $\bullet C_6H_{12}\bullet$ diradical intermediate.

Similar observations have been made in the pyrolysis of 1-hexene by Liu et el. under similar experimental conditions.[14] Although with a different precursor 1-hexene, the $\bullet C_6H_{12}\bullet$ diradical was formed in both cyclohexane and 1-hexene pyrolysis due to isomerization. In that work, the *m*/*z* = 56 peak was found increasing significantly at around 990 K, and it could only be explained by the secondary decompositions of 1,5-

and 1,6- hexyl diradical which were produced from the isomerization reactions of 1-hexene.

The mechanism proposed above that 1,6-hexyl diradical could directly decompose to the *m*/*z* = 56 product was also supported by quantum chemistry investigations carried out in this work. In Figure 4, several possible competing reaction pathways and their energetics that lead to the formation of the *m*/*z* = 56 peak are displayed. The C-C bond

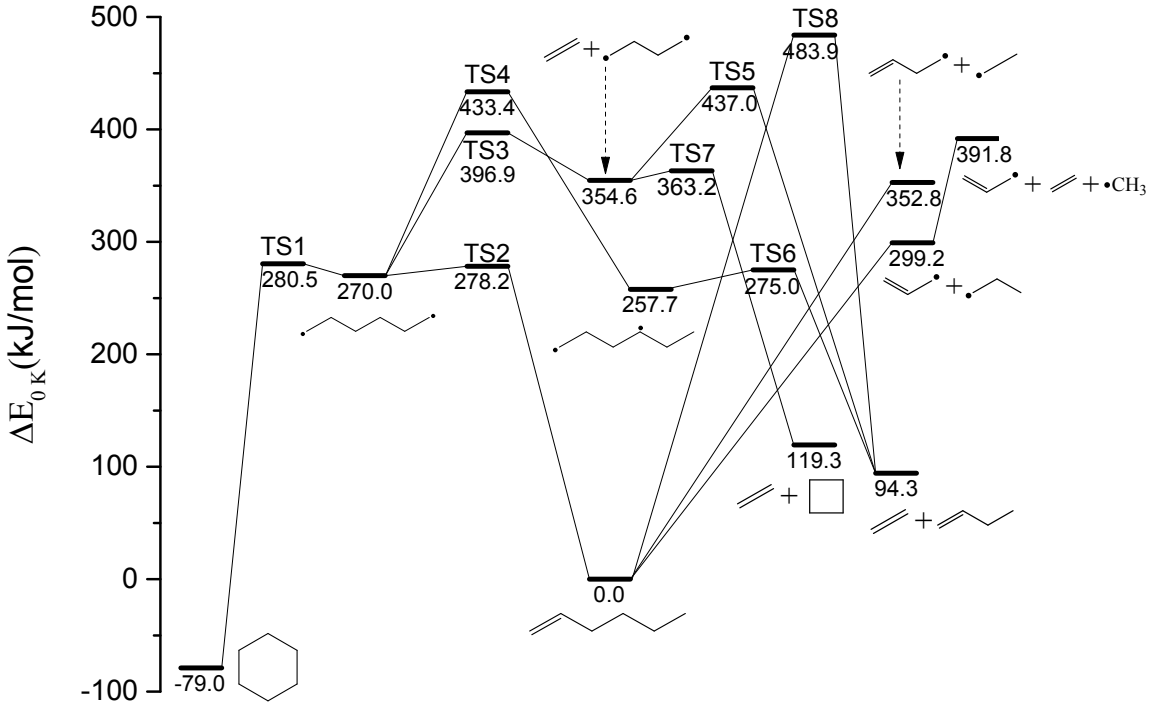

Figure 4. Possible reaction pathways leading to the formation of the *m*/*z* = 56 products, along with some dissociation channels of 1-hexene following isomerization of the 1,6-hexyl diradical. All geometry optimizations and zero-point energy corrections were made at the UB3LYP/cc-pVDZ level. The single-point electronic energies of all species involved were performed at the UCCSD(T)/cc-pVDZ level of theory. The relative energy differences at 0 K were used as the starting reference values.

rupture producing •C_6H_{12}• via TS1 was considered as the initiation step of the cyclohexane decomposition, and the energy barrier was determined to be 359.5 kJ/mol relative to cyclohexane. After the formation of •C_6H_{12}•, 1-hexene could be produced by overcoming TS2 with an 8.2 kJ/mol energy barrier from the 1,6-hexyl diradical intermediate. Figure 4 shows that the isomerization between cyclohexane and 1-hexene can readily take place compared to other reaction pathways. Our theoretical calculations on the initial pathways of 1-hexene isomerization through the 1,6-hexyl diradical intermediate are in agreement with Liu et al. at MRCI(8e,8o)/cc-pVTZ level.[14] In Liu et al., the energy difference between 1-hexene and the 1,6-hexyl diradical was determined to be 278.6 kJ/mol, while in this work the corresponding value is 270.0 kJ/mol. The height of the energy barrier between the transition state TS2 and the 1,6-hexyl diradical was calculated to be 8.8 kJ/mol,[14] similar to 8.2 kJ/mol in this work. The 1,6-hexyl radical could decompose into •C_4H_8• and C_2H_4 through TS3, which requires overcoming an additional barrier of 126.9 kJ/mol (this could take place via thermal activation of the 1,6-hexyl radical by additional collisions with the buffer gas). The •C_4H_8• 1,4-butyl diradical could further take two possible pathways, isomerization to cyclobutane via TS7 with an energy barrier of 8.6 kJ/mol, or formation of 1-butene with a threshold energy of 82.4 kJ/mol via TS5. The detailed geometries of the species involved could be found in the Supplemental Materials.

As the co-product of C_4H_8 in reaction (4), m/z = 28 (C_2H_4) peak seemed to appear around 1070 K and became more obvious at temperatures above 1200K (Figure 2 and 3), although this onset and trend were not well defined. This was possibly because the IE of ethylene (10.51 eV[47]) is slightly higher than the VUV photon energy (10.49 eV), and more significantly because the background signal of N_2^+ made the detection of the ethylene signal difficult. To eliminate the influence of N_2 on the detection of m/z = 28 signal, the pyrolysis of cyclohexane was also performed using helium as a carrier gas under similar thermal decomposition conditions. Without the background signal of N_2 at m/z = 28, the m/z = 28 signal was first detected at about the same temperature where the m/z = 56 species started to be formed. Also, in the mass spectra using the helium carrier gas, the C_2H_4 signal was found to show up at a similar temperature when the m/z = 15 peak appeared, as the secondary decomposition of $\bullet C_3H_7$ producing $\bullet CH_3$ and C_2H_4 could also contribute to the appearance of the m/z = 15 and 28 peaks. In this work, as shown in Figure 2 and 3, the m/z = 15 signal first appeared at 1070 K, which indicated that ethylene could also start to show up at the similar temperature of ~ 1070 K.

In addition to the reaction mechanism mentioned above, several other competing reaction pathways leading to the formation of m/z = 56 species are considered, and the calculated energetics are depicted in Figure 4. The 1,6-hexyl diradical could isomerize to 1,4-hexyl diradical via TS4, followed by 1-butene formation; this reaction pathway requires 163.4 kJ/mol additional energy to go over TS4 from the $\bullet C_6H_{12}\bullet$ diradical. 1-

butene produced directly from 1-hexene via TS8 is also considered; however, the energy threshold is determined to be 483.9 kJ/mol relative to 1-hexene. This reaction channel requires the highest amount of energy, which is the least likely explanation for the *m*/*z* = 56 peak. In summary, according to the theoretical calculations (Figure 4), the most favored pathway for the formation of the C_4H_8 species is that cyclohexane decomposes into the 1,6-hexyl diradical followed by the C2-C3 bond breaking of the 1,6-hexyl diradical in the secondary reaction (likely activated by additional collisions with the buffer gas), which leads to the formation of 1,4-butyl diradical. Then the 1,4-butyl diradical could isomerize to cyclobutane via TS7 or to 1-butene via TS5. Although the formation of 1-hexene was the reaction channel with the lowest energy barrier among the secondary reactions of the $\bullet C_6H_{12}\bullet$ diradical, the formation of *m*/*z* = 56 could not be readily explained by the direct dissociation of 1-hexane due to the high energy barrier of TS8. And this supports the conclusion in the previous investigation carried by Liu et al. that 1-hexene has to go through the $\bullet C_6H_{12}\bullet$ diradical to form the C_4H_8 species.[14]

In Sirjean et al., the rate constants for different potential pathways of the 1,6-hexyl diradical were determined at 1 atm pressure, from 600 K to 2000 K.[26] Under such condition, the reaction of the 1,6-hexyl diradical leading to 1-hexene was considered to be more important than that to the C_4H_8 species, as the C_4H_8 species had not been observed as a unimolecular dissociation product previously.[6, 26] In this work, thermal decomposition production of the C_4H_8 species was identified. However, it was difficult

and inconclusive to quantify the kinetics in this work, due to the complexity in the experimental conditions (e.g., non-uniformity of pressure and temperature). Therefore, this work mainly focused on the qualitative analysis of the kinetics in the microreactor.

1.2 Decomposition of 1-hexene formed from cyclohexane isomerization

Cyclohexane isomerizing to 1-hexene is an important mechanism in the thermal dissociation of cyclohexane. Several mass peaks likely produced from the decomposition of 1-hexene were also identified in this work. Figure 1 and 2 show that when the temperature reached ~1070 K, the peaks at m/z = 41 and 42 started to appear and grew significantly at higher temperatures, indicating the production of $\bullet C_3H_5$ and C_3H_6. The peak area ratio of m/z 41/84 ($\bullet C_3H_5$ versus C_6H_{12}) in Figure 3 was nearly constant below 1070 K and started to increase at around 1070 K. The formation of the m/z = 41 peak ($\bullet C_3H_5$) is known from the following steps: cyclohexane first isomerizes to 1-hexene via the diradical intermediate (reaction (1)), then 1-hexene undergoes C3-C4 bond homolysis (reaction (2)). $\bullet C_3H_5$ was less likely to be produced via H-loss secondary reaction from the propene product under our experimental condition, as propene has a strong C-H bond.[6, 9, 13, 15] According to Figure 1 and 2, the signal m/z = 43 ($\bullet C_3H_7$), which was the counterpart of $\bullet C_3H_5$ in reaction (2), was detected with a minor amount at 1070 K. It increased more at ~ 1150 K but remained very small. This was possibly due to the unstable nature of the *n*-propyl radical $\bullet C_3H_7$, which further decomposed rapidly into methyl

radical and ethylene (reaction (14)) or, to a lesser extent, propene and H (reaction (15)).[13, 14, 48, 49] The observation of the *m*/*z* = 15 peak at 1070 K, as well as the arguments mentioned previously that ethylene was captured at around 1070 K, was consistent with the assumption that $\bullet C_3H_7$ was unstable and decomposed rapidly.

$$\bullet C_3H_7 \rightarrow \bullet CH_3 + C_2H_4 \quad (14)$$

$$\bullet C_3H_7 \rightarrow H\bullet + C_3H_6 \quad (15)$$

As shown in the mass spectra in Figure 2 and peak area ratio of *m*/*z* 42/84 in Figure 3, the *m*/*z* = 42 species were produced at ~1070 K. There are several possible sources of C_3H_6 formation. It could be evolved from 1-hexene after the initial isomerization from cyclohexane, which decomposed through a retro-ene mechanism into two propene molecules (reaction (3)),[6, 14, 50] although this was later considered to be not important.[13, 14] It could also be originated from the $\bullet C_6H_{12}\bullet$ diradical as described in reaction (5): cyclohexane first broke a C-C bond forming the 1,6-hexyl diradical followed by isomerization to 1,5-hexyl diradical or 2,5-hexyl diradical, leading to propene plus cyclopropane or two propene molecules via symmetric C-C breaking, or the symmetric C-C bond breaking of the 1,6-hexyl diradical could directly lead to the formation of two cyclopropane (reaction (16)).[13, 14, 26] As discussed earlier, to a lesser extent, it was also possible to be produced from the secondary decomposition of the n-propyl radical, losing one H to form propene (reaction (15)).

$$c\text{-}C_6H_{12} \leftrightarrow \bullet CH_2(CH_2)_4H_2C\bullet \rightarrow 2\ c\text{-}C_3H_6 \quad (16)$$

Some other reaction products associated with 1-hexene following the isomerization of cyclohexane through the 1,6-hexyl diradical (reaction (1)) was observed. The m/z = 55 peak, which corresponds to $\bullet C_4H_7$, was found to increase significantly at around 1070 K, and its intensity kept nearly constant until the temperature reached around 1310 K as shown in Figure 1 and 2. It was likely produced by the C4-C5 bond fission of 1-hexene. It could also be produced from the H-loss secondary reactions of 1-butene at high temperatures. The co-product of $\bullet C_4H_7$ in reaction (11), $\bullet C_2H_5$ (m/z = 29), was not observed at all temperatures, although its ionization energy is 8.12 eV,[51] below the 10.49 eV VUV photon energy in this work. This was probably caused by the fast dissociation of $\bullet C_2H_5$ which led to the formation of C_2H_4 + H.[52] According to Figure 1 and 2, at 1150 K, m/z = 68 was first observed, and its intensity kept almost constant when the temperature further increased. The m/z = 68 peak was possibly the H-loss reaction product of $\bullet C_5H_9$ radical, which could be produced in reaction (12) from 1-hexene. There was a very minor amount of m/z = 69 signal around these temperatures.

The decomposition channels of 1-hexene were also examined theoretically. The DFT calculations on some of the dissociation channels of 1-hexene are presented in Figure 4. It shows that reaction (2) only requires an additional energy barrier of 299.2 kJ/mol

relative to 1-hexene which makes it the most competitive dissociation channel among all, while reaction (11) has an energy barrier of 352.8 kJ/mol. Those two reaction channels have lower energy thresholds than the lowest possible threshold energy of the formation of the m/z = 56 species. The further secondary reaction of the $\bullet C_3H_7$ radical producing C_2H_4 and $\bullet CH_3$ is displayed with its energetics in Figure 4 as well. An additional 92.6 kJ/mol energy barrier needs to be overcome for the $\bullet C_3H_7$ radical, which makes the overall energy barrier for the formation of ethylene + $\bullet CH_3$ to be around 470.8 kJ/mol from cyclohexane. Note that this energy is about the same as the overall energy barrier of TS3 (475.9 kJ/mol relative to cyclohexane), which leads to the C_4H_8 product. The observation of the ethylene + $\bullet CH_3$ products and the C_4H_8 product around the same onset temperature in this work was consistent with these two similar energy barriers.

The theoretical investigations along with the experimental observations discussed above suggested that the predominant thermal decomposition reaction channels of cyclohexane pyrolysis were carried out via 1-hexene. This is consistent with previous investigations on the thermal decomposition of cyclohexane and 1-hexene, in which both species show many features in common in their pyrolysis processes. However, the secondary reactions of the hexyl-diradicals were often omitted, and in this work, both experimental and theoretical studies have shown that the secondary reactions of the 1,6-hexyl diradical are important among the unimolecular reactions. Consequently, the

impact of the diradicals on the overall pyrolysis mechanism of similar cycloalkane systems needs to be evaluated.

1.3 Other initiation channels of cyclohexane

At all temperatures in this work, m/z = 83 peak ($\bullet C_6H_{11}$) was not detected. However, $\bullet C_6H_{11}$ has an ionization energy of 7.66 eV[53] and can be detected by the 10.49 eV VUV laser radiation used in this work, and it was detected in the pyrolysis of methylcyclohexane under the similar experimental conditions.[54] Therefore, H-atom loss (reaction (9)) was not one of the initiation steps of cyclohexane pyrolysis. This is understandable because the C-H bond (~410.9 kJ/mol) is much stronger than the C-C bond (~346.0 kJ/mol) in cyclohexane, which required more energy to break among the primary dissociation pathways under the unimolecular decomposition conditions. The cyclohexyl radical observed in some of the earlier studies under different conditions was likely produced from bimolecular reactions.[13, 15] In return, the absence of the m/z = 83 cyclohexyl signal in this work confirmed that bimolecular reactions were indeed minimized under the current experimental conditions.

When the temperature reached 1120 K, the m/z = 82 peak started to appear, and it most likely represented the signal of cyclohexene. According to the discussion above, cyclohexene was produced by the H_2 elimination reaction of cyclohexane (reaction (10)). When the temperature reached 1190 K and above, m/z = 80 and 78 started to appear

subsequently, and *m*/*z* = 78 kept growing as the temperature increased. As shown in Figure 1 and 2, the signals of further H_2 elimination products such as *m*/*z* = 76 or 74 were not observed, which indicated that *m*/*z* = 78 was very stable at high temperatures and unlikely to be an open-chain unsaturated hydrocarbon. This further supports that the *m*/*z* = 78 product likely corresponded to benzene. As the bimolecular reactions were minimized under the current experimental conditions, benzene at *m*/*z* = 78 was not likely produced from recombination of small fragments, and therefore, it should be formed from sequential H_2 eliminations (reaction (17)), while the cyclohexyl radical was not detected.

$$c\text{-}C_6H_{12} \xrightarrow{-H_2} c\text{-}C_6H_{10} \xrightarrow{-H_2} c\text{-}C_6H_8 \xrightarrow{-H_2} C_6H_6 \quad (17)$$

2. Secondary reactions in cyclohexane pyrolysis

The decomposition fragments of cyclohexane after the initiation reactions went through a series of secondary reactions. The *m*/*z* = 40 and 39 peaks, which first showed up after 1120 K, were produced by the secondary reactions of the allyl radical and propene. The energetics of allyl radicals and propene have been examined theoretically and experimentally previously.[55, 56] Besides the pathways that lead to the formation of the C_3H_4 and C_3H_3 species, allyl radical could also decompose into C_2H_2 and $\bullet CH_3$

radical.[56] The m/z = 54 peak first appeared at 1070 K and it represented 1,3-butadiene. The m/z = 52 peak represented 1-buten-3-yne (or cyclobutadiene) and it was first observed at 1190 K. The peak intensities of these two peaks increased as the temperature further increased. They were evolved from sequential H_2 loss of C_4H_8 (1-butene or cyclobutane) or H-loss of the $\bullet C_4H_7$ radical. Also, the secondary decomposition of cyclohexene could contribute to the yields of 1,3-butadiene (known as retro-Diels Alder mechanism).[34] The m/z = 68 (C_5H_8) and 66 (C_5H_6) peaks, which were first observed at around 1190 K, could be explained by the secondary reactions of $\bullet C_5H_9$ radical produced in reaction (12). To summarize, important initiation steps and part of the secondary reactions for the thermal decomposition of cyclohexane are depicted in Scheme 3.

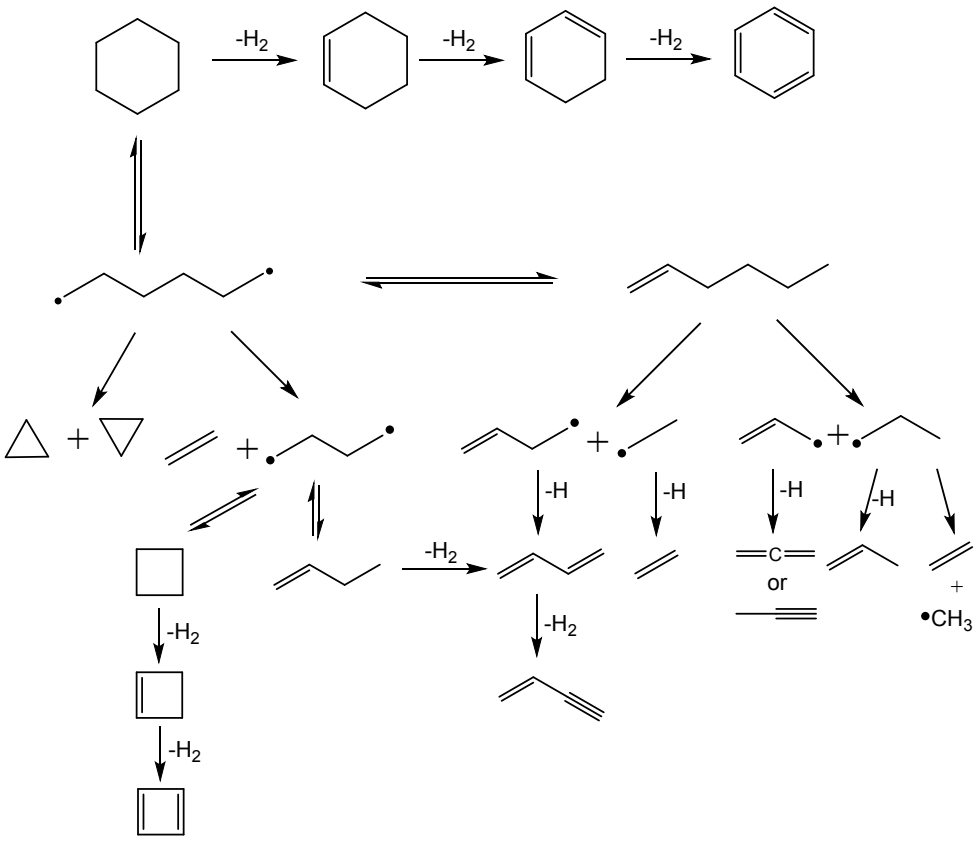

Scheme 3. Main initiation decomposition mechanism of cyclohexane.

Conclusion

The thermal decomposition of cyclohexane was studied by flash pyrolysis coupled with molecular beam sampling and VUV-PI-MS in this work. The C-C bond rupture of cyclohexane producing the 1,6-hexyl diradical was the main initiation reaction pathway. The $m/z = 56$ species was produced primarily by the direct dissociation reaction of the 1,6-hexyl diradical under unimolecular reaction conditions, and it was unlikely to be formed through 1-hexene which was the important isomerization product of the 1,6-hexyl diradical. Experimental observations and quantum chemistry investigations in this work

were consistent with this mechanism. This work also shows that the pyrolysis of cyclohexane did not produce the $\bullet C_6H_{11}$ radical by C-H bond fission. Direct evidence for the sequential H_2 eliminations to form m/z = 82 (c-C_6H_{10}), 80 (c-C_6H_8), and 78 (benzene) were found.

This work, as well as the previous work on the 1-hexene and 1-heptene pyrolysis by Liu et al.,[14] have demonstrated the significance of the direct dissociation pathways of hydrocarbon diradicals and can provide insight into further numerical modeling studies on similar cycloalkane systems.

Acknowledgment

This work was supported by the US National Science Foundation (CHE-1566636). Xinghua Liu acknowledges support of a scholarship from China Scholarships Council (201606440042).

References:

1. G. W. Huber, S. Iborra and A. Corma, *Chemical Reviews*, 2006, **106**, 4044-4098.
2. A. M. Mastral and M. S. Callén, *Environmental Science & Technology*, 2000, **34**, 3051-3057.
3. E. Ranzi, A. Cuoci, T. Faravelli, A. Frassoldati, G. Migliavacca, S. Pierucci and S. Sommariva, *Energy & Fuels*, 2008, **22**, 4292-4300.
4. W. Jin, L. Pastor-Pérez, D. Shen, A. Sepúlveda-Escribano, S. Gu and T. Ramirez Reina, *ChemCatChem*, 2019, **11**, 924-960.
5. L. Mo, W. Yu, H. Cai, H. Lou and X. Zheng, *Frontiers in Chemistry*, 2018, **6**, 1-8.
6. W. Tsang, *International Journal of Chemical Kinetics*, 1978, **10**, 1119-1138.
7. T. C. Brown, K. D. King and T. T. Nguyen, *The Journal of Physical Chemistry*, 1986, **90**, 419-424.
8. D. S. Aribike and A. A. Susu, *Applied Petrochemical Research*, 2018, **8**, 193-201.
9. D. S. Aribike, A. A. Susu and A. F. Ogunye, *Thermochimica Acta*, 1981, **51**, 113-127.
10. A. El Bakali, M. Braun-Unkhoff, P. Dagaut, P. Frank and M. Cathonnet, *Proceedings of the Combustion Institute*, 2000, **28**, 1631-1638.
11. U. Steil, M. Braun-Unkhoff, C. Naumann and P. Frank, in *Proceedings of the European Combustion Meeting*, Louvain-la-Neuve, Belgium, April 3–6, 2005.
12. S. Granata, T. Faravelli and E. Ranzi, *Combustion and Flame*, 2003, **132**, 533-544.
13. J. H. Kiefer, K. S. Gupte, L. B. Harding and S. J. Klippenstein, *The Journal of Physical Chemistry A*, 2009, **113**, 13570-13583.
14. X. Liu, W. Yuan, J. Zhang, J. Yang and Z. Zhou, *Proceedings of the Combustion Institute*, 2020, https://doi.org/10.1016/j.proci.2020.1007.1060.

15. Z. Wang, Z. Cheng, W. Yuan, J. Cai, L. Zhang, F. Zhang, F. Qi and J. Wang, *Combustion and Flame*, 2012, **159**, 2243-2253.

16. S. Peukert, C. Naumann, M. Braun-Unkhoff and U. Riedel, *International Journal of Chemical Kinetics*, 2011, **43**, 107-119.

17. I. G. Zsély, T. Varga, T. Nagy, M. Cserháti, T. Turányi, S. Peukert, M. Braun-Unkhoff, C. Naumann and U. Riedel, *Energy*, 2012, **43**, 85-93.

18. M. K. Liszka and K. Brezinsky, *International Journal of Chemical Kinetics*, 2019, **51**, 49-73.

19. D. Voisin, A. Marchal, M. Reuillon, J. C. Boettner and M. Cathonnet, *Combustion Science and Technology*, 1998, **138**, 137-158.

20. O. Lemaire, M. Ribaucour, M. Carlier and R. Minetti, *Combustion and Flame*, 2001, **127**, 1971-1980.

21. F. Billaud, P. Chaverot, M. Berthelin and E. Freund, *Industrial & Engineering Chemistry Research*, 1988, **27**, 759-764.

22. W. Li, M. E. Law, P. R. Westmoreland, T. Kasper, N. Hansen and K. Kohse-Höinghaus, *Combustion and Flame*, 2011, **158**, 2077-2089.

23. C. S. McEnally and L. D. Pfefferle, *Combustion and Flame*, 2004, **136**, 155-167.

24. K. H. Weber and J. Zhang, *The Journal of Physical Chemistry A*, 2007, **111**, 11487-11492.

25. M. V. Khandavilli, M. Djokic, F. H. Vermeire, H.-H. Carstensen, K. M. Van Geem and G. B. Marin, *Energy & Fuels*, 2018, **32**, 7153-7168.

26. B. Sirjean, P. A. Glaude, M. F. Ruiz-Lopez and R. Fournet, *The Journal of Physical Chemistry A*, 2006, **110**, 12693-12704.

27. C.-M. Gong, Z.-R. Li and X.-Y. Li, *Energy & Fuels*, 2012, **26**, 2811-2820.

28. X. Huang, D. Cheng, F. Chen and X. Zhan, *Journal of Energy Chemistry*, 2015, **24**, 65-71.

29. K. Shao, Y. Tian and J. Zhang, *International Journal of Mass Spectrometry*, 2021, **460**, 116476-116484.

30. X. Liu, J. Zhang, A. Vazquez, D. Wang and S. Li, *The Journal of Physical Chemistry A*, 2019, **123**, 10520-10528.

31. S. D. Chambreau, J. Zhang, J. C. Traeger and T. H. Morton, *International Journal of Mass Spectrometry*, 2000, **199**, 17-27.

32. D. W. Kohn, H. Clauberg and P. Chen, *Review of Scientific Instruments*, 1992, **63**, 4003-4005.

33. M. V. Zagidullin, R. I. Kaiser, D. P. Porfiriev, I. P. Zavershinskiy, M. Ahmed, V. N. Azyazov and A. M. Mebel, *The Journal of Physical Chemistry A*, 2018, **122**, 8819-8827.

34. Q. Guan, K. N. Urness, T. K. Ormond, D. E. David, G. Barney Ellison and J. W. Daily, *International Reviews in Physical Chemistry*, 2014, **33**, 447-487.

35. P. J. Jones, B. Riser and J. Zhang, *The Journal of Physical Chemistry A*, 2017, **121**, 7846-7853.

36. K. H. Weber, J. M. Lemieux and J. Zhang, *The Journal of Physical Chemistry A*, 2009, **113**, 583-591.

37. E. Kraka and D. Cremer, *Journal of the American Chemical Society*, 2000, **122**, 8245-8264.

38. D. H. Ess, E. R. Johnson, X. Hu and W. Yang, *The Journal of Physical Chemistry A*, 2011, **115**, 76-83.

39. T. Ziegler, A. Rauk and E. J. Baerends, *Theoretica chimica acta*, 1977, **43**, 261-271.

40. P. Sinha, S. E. Boesch, C. Gu, R. A. Wheeler and A. K. Wilson, *The Journal of Physical Chemistry A*, 2004, **108**, 9213-9217.

41. G. W. T. M. J. Frisch, H. B. Schlegel, G. E. Scuseria, M. A. Robb, J. R. Cheeseman, G. Scalmani, V. Barone, B. Mennucci, G. A. Petersson, H. Nakatsuji, M. Caricato, X. Li, H. P. Hratchian, A. F. Izmaylov, J. Bloino, G. Zheng, J. L. Sonnenberg, M. Hada, M. Ehara, K. Toyota, R. Fukuda, J. Hasegawa, M. Ishida, T. Nakajima, Y. Honda, O. Kitao, H. Nakai, T. Vreven, J. A. Montgomery, Jr., J. E. Peralta, F. Ogliaro, M. Bearpark, J. J. Heyd, E. Brothers, K. N. Kudin, V. N. Staroverov, R. Kobayashi, J. Normand, K. Raghavachari, A. Rendell, J. C. Burant, S. S. Iyengar, J. Tomasi, M. Cossi, N. Rega, J. M. Millam, M. Klene, J. E. Knox, J. B. Cross, V. Bakken, C. Adamo, J. Jaramillo, R. Gomperts, R. E. Stratmann, O. Yazyev, A. J. Austin, R. Cammi, C. Pomelli, J. W. Ochterski, R. L. Martin, K. Morokuma, V. G. Zakrzewski, G. A. Voth, P. Salvador, J. J. Dannenberg, S. Dapprich, A. D. Daniels, Ö. Farkas, J. B. Foresman, J. V. Ortiz, J. Cioslowski, and D. J. Fox, *Gaussian 09*, (2009), Wallingford, CT.

42. J. Meija, B. Coplen Tyler, M. Berglund, A. Brand Willi, P. De Bièvre, M. Gröning, E. Holden Norman, J. Irrgeher, D. Loss Robert, T. Walczyk and T. Prohaska, *Pure and Applied Chemistry*, 2016, **88**, 265-291.

43. L. W. Sieck and M. Mautner, *The Journal of Physical Chemistry*, 1982, **86**, 3646-3650.

44. Y. L. Sergeev, M. E. Akopyan, F. I. Vilesov and Y. V. Chizhov, *High Energy Chem.*, 1973, **369**, 418 in original.

45. M. Grade, J. Wienecke, W. Rosinger and W. Hirschwald, *Berichte der Bunsengesellschaft für physikalische Chemie*, 1983, **87**, 355-361.

46. S. D. Chambreau, J. Lemieux, L. Wang and J. Zhang, *The Journal of Physical Chemistry A*, 2005, **109**, 2190-2196.

47. K. Ohno, K. Okamura, H. Yamakado, S. Hoshino, T. Takami and M. Yamauchi, *The Journal of Physical Chemistry*, 1995, **99**, 14247-14253.

48. L. E. Gusel'nikov, V. V. Volkova, P. E. Ivanov, S. V. Inyushkin, L. V. Shevelkova, G. Zimmermann, U. Ziegler and B. Ondruschka, *Journal of Analytical and Applied Pyrolysis*, 1991, **21**, 79-93.

49. V. V. Volkova, L. E. Gusel'nikov and G. Zimmermann, *Journal of Analytical and Applied Pyrolysis*, 1992, **23**, 265-286.

50. M. Yahyaoui, N. Djebaïli-Chaumeix, C. E. Paillard, S. Touchard, R. Fournet, P. A. Glaude and F. Battin-Leclerc, *Proceedings of the Combustion Institute*, 2005, **30**, 1137-1145.

51. B. Ruscic, J. Berkowitz, L. A. Curtiss and J. A. Pople, *The Journal of Chemical Physics*, 1989, **91**, 114-121.

52. A. F. Wagner, L. A. Rivera-Rivera, D. Bachellerie, J. W. Perry and D. L. Thompson, *The Journal of Physical Chemistry A*, 2013, **117**, 11624-11639.

53. R. F. Pottie, A. G. Harrison and F. P. Lossing, *Journal of the American Chemical Society*, 1961, **83**, 3204-3206.

54. K. H. Weber, University of California, Riverside 2010.

55. F. H. Vermeire, R. De Bruycker, O. Herbinet, H.-H. Carstensen, F. Battin-Leclerc, G. B. Marin and K. M. Van Geem, *Fuel*, 2017, **208**, 779-790.

56. B. S. Narendrapurapu, A. C. Simmonett, H. F. Schaefer, J. A. Miller and S. J. Klippenstein, *The Journal of Physical Chemistry A*, 2011, **115**, 14209-14214.